Hydrogen-Bonding Cavities about Metal Ions: Synthesis, Structure, and Physical Properties for a Series of Monomeric M−OH Complexes Derived from Water

Cora E. MacBeth,[†] Brian S. Hammes,[†] Victor G. Young, Jr.,[‡] and A. S. Borovik*[,†]

Department of Chemistry, University of Kansas, Lawrence, Kansas 66045, and Department of Chemistry, University of Minnesota, Minneapolis, Minnesota 55455

Received March 6, 2001

The tripodal ligand $N[CH_2CH_2NHC(O)NHC(CH_3)_3]_3$ ($[H_6\mathbf{1}]$) was used to synthesize a series of monomeric complexes with terminal hydroxo ligands. The complexes $[Co^{II/III}H_3\mathbf{1}(OH)]^{2-/1-}$, $[Fe^{II/III}H_3\mathbf{1}(OH)]^{2-/1-}$, and $[Zn^{II}H_3\mathbf{1}(OH)]^{2-}$ have been isolated and characterized. The source of the hydroxo ligand in these complexes is water, which was confirmed with an isotopic labeling study for $[Co^{III}H_3\mathbf{1}(OH)]^{1-}$. The synthesis of $[M^{II}H_3\mathbf{1}(OH)]^{2-}$ complexes was accomplished by two routes. Method A used 3 equiv of base prior to metalation and water binding, affording yields of ≤40% for $[Co^{II}H_3\mathbf{1}(OH)]^{2-}$. When 4 equiv of base was used (method B), yields ranged from 50% to 70% for all of the $M^{II}H_3\mathbf{1}(OH)]^{2-}$ complexes. This improvement is attributed to the presence of an intramolecular basic site within the cavity, which scavenges protons produced during formation of the M^{II}−OH complexes. The molecular structures of $[Zn^{II}H_3\mathbf{1}(OH)]^{2-}$, $[Fe^{II}H_3\mathbf{1}(OH)]^{2-}$, $[Co^{II}H_3\mathbf{1}(OH)]^{2-}$, and $[Co^{III}H_3\mathbf{1}(OH)]^{1-}$ were examined by X-ray diffraction methods. The complexes have trigonal bipyramidal coordination geometry with the hydroxo oxygen trans to the apical nitrogen. The three M^{II}−OH complexes crystallized with nearly identical lattice parameters, and each contains two independent anions in the asymmetric unit. The complexes have intramolecular H-bonds from the urea cavity of $[H_3\mathbf{1}]^{3-}$ to the coordinated hydroxo oxygen. All the complexes have long M−O(H) bond lengths (>2.00 Å) compared to those of the few previously characterized synthetic examples. The longer bond distances in $[M^{II}H_3\mathbf{1}(OH)]^{2-}$ reflect the intramolecular H-bonds in the complexes. The five-coordinate $[Zn^{II}H_3\mathbf{1}(OH)]^{2-}$ has an average Zn−O(H) distance of 2.024(2) Å, which is similar to that found for the zinc site in carbonic anhydrase II (2.05(2) Å). The enzyme active site also has an extensive network of intramolecular H-bonds to the hydroxo oxygen. $[Co^{II}H_3\mathbf{1}(OH)]^{2-}$ and $[Fe^{II}H_3\mathbf{1}(OH)]^{2-}$ have one-electron redox processes at −0.74 and −1.40 V vs SCE. Both complexes can be chemically oxidized to yield their corresponding M^{III}−OH complexes. $[Co^{III}H_3\mathbf{1}(OH)]^{1-}$, with an $S = 1$ ground state, is a rare example of a paramagnetic Co^{III} complex.

Introduction

Metal centers with terminal hydroxo ligands are important functional units in metalloproteins. M−OH units are proposed as the active species in a wide variety of proteins including zinc and nickel hydrolytic enzymes,[1] iron and cobalt nitrile hydratases,[2] iron-containing lipoxygenases[3] and acid phosphatases,[4] and intermediate states in the oxygen-evolving complex[5] in photosynthesis. In these enzymes, the terminal hydroxo ligand is generated from water. X-ray diffraction studies on many of these enzymes suggest that there are functional groups positioned within the active site that are essential for function.[1,4] Two types of functional groups are most commonly found near the M−OH units. The first are basic functionalities, such as carboxylates, which serve as endogenous bases to scavenge protons liberated during the formation of M−OH centers. The second group is comprised of amino acid residues that can provide hydrogen bond(s) to the terminal hydroxo ligand. Both aid in regulating the activity of the M−OH unit while adding structural stability to the active site.

Difficulties in duplicating these structural properties in synthetic systems have led to few reports of monomeric $Fe^{II/III}$,[6−8] $Co^{II/III}$,[9,10] and Zn^{II} complexes[11] with terminally

[†] University of Kansas.
[‡] University of Minnesota.

(1) (a) Dixon, N. E.; Riddles, P. W.; Gazzola, C.; Blakeley, R. L.; Zerner, B. *Can. J. Biochem.* **1980**, *58*, 1335−1344. (b) Jabri, E.; Carr, M. B.; Hausinger, R. P.; Karplus, P. A. *Science* **1995**, *268*, 998−1004. (c) Lipscomb, W. N.; Sträter, N. *Chem. Rev.* **1996**, *96*, 2375−2433 and references therein. (d) Christianson, D. W.; Cox, J. D. *Annu. Rev. Biochem.* **1999**, *68*, 33−57. (e) Christianson, D. W.; Fierke, C. A. *Acc. Chem. Res.* **1996**, *29*, 331−339.

(2) (a) Huang, W.; Jia, J.; Cumming, J.; Nelson, M.; Schneider, G.; Lindqvist, Y. *Structure* **1997**, *5*, 691−699. (b) Scarrow, R. C.; Brennan, B. A.; Cummings, J. G.; Jin, H.; Duong, D. J.; Kindt, J. T.; Nelson, M. J. *Biochemistry* **1996**, *35*, 10078−10088. (c) Brennan, B. A.; Alms, G.; Nelson, M. J.; Durney, L. T.; Scarrow, R. C. *J. Am. Chem. Soc.* **1996**, *118*, 9194−9195.

(3) Selected papers: (a) Nelson, M. J. *J. Am. Chem. Soc.* **1988**, *110*, 2985−2986. (b) Scarrow, R. C.; Trimitsis, M. G.; Buck, C. P.; Grove, G. N.; Cowling, R. A.; Nelson, M. J. *Biochemistry* **1994**, *33*, 15219−15229.

(4) (a) Wilcox, D. E. *Chem. Rev.* **1996**, *96*, 2435−2458. (b) Klabunde, T.; Sträter, N.; Fröhlich, R.; Witzel, H.; Krebs, B. *J. Mol. Biol.* **1996**, *259*, 737−748.

(5) Hoganson, C. W.; Babcock, G. T. *Science* **1997**, *277*, 1953−1956.

(6) Fe^{II}−OH: Hikichi, S.; Ogihara, T.; Fujisawa, K.; Kitajima, N.; Akita, M.; Moro-oko, Y. *Inorg. Chem.* **1997**, *36*, 4539−4547.

(7) Non-heme Fe^{III}−OH: Ogo, S.; Wada, S.; Watanabe, Y.; Iwase, M.; Wada, A.; Harata, M.; Jitsukawa, K.; Masuda, H.; Einaga, H. *Angew. Chem., Int. Ed.* **1998**, *37*, 2102−2104.

(8) Heme Fe^{III}−OH: Yeh, C.-Y.; Chang, C. J.; Nocera, D. G. *J. Am. Chem. Soc.* **2001**, *123*, 1513−1514.

(9) Co^{II}−OH: Orlandini, A.; Sacconi, L. *Inorg. Chem.* **1976**, *15*, 78−85.

(10) Co^{III}−OH: Kucharski, S. E.; Skelton, B. W.; White, A. H. *Aust. J. Chem.* **1978**, *31*, 47−51.

10.1021/ic010250w CCC: $20.00
Published on Web 07/31/2001

coordinated hydroxo ligands. Multinuclear complexes with $M-(OH)_n-M$ cores are often obtained because of the propensity of the hydroxo ligand to bridge between metal ions. Furthermore, the inability of synthetic complexes to correctly position basic groups and H-bonds near metal centers has resulted in inadequate regulation of the secondary coordination sphere, as compared to those found in metalloproteins.

Our group, along with those of Masuda[7,12,13] and Berreau,[14] has developed tripodal ligands that place H-bonding groups near a metal center in monomeric complexes.[15] We use the ligand tris[(*N*′-*tert*-butylureayl)-*N*-ethyl]amine ([H_6**1**]), which contains

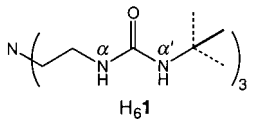

H_6**1**

three urea groups appended from a central amine nitrogen via ethylene spacers.[16] Deprotonation of the α nitrogens leads to the trianionic ligand $[H_3\mathbf{1}]^{3-}$ that readily binds metal ions. This binding creates a protective H-bonding cavity around the metal center that is provided by the three α′-NHR groups of the ligand. Intramolecular H-bonds between the cavity α′-NH groups and the atom coordinating to the metal center occur because thermodynamically favored six-membered rings are formed when these interactions take place. We have recently found that additional deprotonation of one α′-NH group leads to metal complexes with an intramolecular base positioned within the cavity.[16c] The presence of this additional basic site can act to scavenge protons, which allows for the increased yields of some monomeric products. Application of this synthetic method to the formation of monomeric $[M^{II}H_3\mathbf{1}(OH)]^{2-}$ complexes (M^{II} = Fe^{II}, Co^{II}, Zn^{II}) derived from water is reported. In addition, the $Fe^{II}-OH$ and $Co^{II}-OH$ complexes can be readily oxidized to yield the corresponding $[M^{III}H_3\mathbf{1}(OH)]^{1-}$ species. Their structural and physical properties, along with those of the monomeric $M^{II}-OH$ complexes, are described. A preliminary account of this work has previously been reported.[16a]

Experimental Section

Preparative Methods and Syntheses. All reagents were purchased from commercial sources and used as received, unless otherwise noted. Anhydrous solvents were purchased from Aldrich. Dioxygen was dried on a Drierite gas purifier that was purchased from Fisher Scientific. The syntheses of all metal complexes were conducted in a Vacuum Atmosphere drybox under an argon atmosphere. Elemental analyses of all compounds were performed at Desert Analytics, Tucson, AZ. All samples were dried in vacuo before analysis. The presence of solvates was corroborated by FTIR and ^{1}H NMR spectroscopy. H_6**1** was synthesized using literature methods.[16b,c] The syntheses of $K_2[Co^{II}H_3\mathbf{1}(OH)]$ by method A and $K[Co^{III}H_3\mathbf{1}(OH)]$ have been reported previously[16a] and are included here, in part, for completeness.

Synthesis of $M^{II}-OH$ Complexes: Method A. Potassium {Tris[(*N*′-*tert*-butylureaylato)-*N*-ethyl]aminato(hydroxo)}-cobaltate(II) ($K_2[Co^{II}H_3\mathbf{1}(OH)]$).[16a] A solution of H_6**1** (0.11 g, 0.24 mmol) in 4 mL of anhydrous DMA was treated with solid KH (0.028 g, 0.72 mmol) under an Ar atmosphere. After H_2 evolution had ceased, $Co(OAc)_2$ (0.043 g, 0.24 mmol) was added as a solid. The resulting solution was stirred for 0.5 h and filtered to remove a small amount of insoluble material (KOAc) which was discarded. H_2O (0.0090 g, 0.48 mmol) was added to the filtrate, and the addition caused an immediate color change from blue to violet. The reaction mixture was stirred for 1 h and filtered. The violet filtrate was crystallized by vapor diffusion of diethyl ether into a DMA solution of $K_2[CoH_3\mathbf{1}(OH)]$ (0.068 g, 40% yield). Anal. Calcd (found) for $K_2[CoH_3\mathbf{1}(OH)]\cdot 0.75DMA$, $C_{24}H_{46.5}CoK_2N_{7.75}O_{4.5}$ (includes 0.75 DMA): C, 42.99 (43.24); H, 7.50 (7.86); N, 16.71 (16.30). IR (Nujol, cm^{-1}): the $\nu(Co^{II}O-H)$ was not observed, ν(NH) 3227, 3138 (urea, s), ν(CO) 1587 (urea, vs). EPR (X-band, DMA, 77 K): $g = 3.87$. UV/vis (DMA): $\lambda_{max}(\epsilon) = 395$ (sh), 474 (sh), 514 (52), 596 (sh), 618 (sh), 681 (24).

Synthesis of $M^{II}-OH$ Complexes: Method B. Potassium {Tris-[(*N*′-*tert*-butylureaylato)-*N*-ethyl]aminato(hydroxo)}ferrate(II) ($K_2[Fe^{II}H_3\mathbf{1}(OH)]$). A solution of H_6**1** (0.117 g, 0.264 mmol) in 10 mL of anhydrous DMA was treated with solid KH (0.042 g, 1.1 mmol) under an argon atmosphere. After gas evolution ceased, solid $Fe(OAc)_2$ (0.046 g, 0.26 mmol) was added in one portion and the mixture was stirred for 15 min. The reaction mixture was then filtered to remove KOAc (0.051 g, 0.53 mmol). The resulting filtrate was treated with 1 equiv of H_2O (4.8 μL, 0.26 mmol) and stirred for 30 min. The reaction mixture was concentrated to dryness under reduced pressure to yield 0.174 g (74%) of $K_2[Fe^{II}H_3\mathbf{1}(OH)]$ as a pale yellow solid. $K_2[Fe^{II}H_3\mathbf{1}(OH)]$ was crystallized by vapor diffusion of diethyl ether into a DMA solution of the salt. The light yellow crystals were isolated, washed with diethyl ether, and dried under vacuum to yield 0.121 g (61%) of the desired salt. Anal. Calcd (found) for $K_2[Fe^{II}H_3\mathbf{1}(OH)]\cdot 1.5DMA$, $C_{27}H_{56.5}FeK_2N_{8.5}O_{5.5}$: C, 44.90 (44.96); H, 7.88 (7.78); N, 16.48 (15.90). FTIR (Nujol, cm^{-1}): the $\nu(Fe^{II}O-H)$ was not observed, ν(NH) 3223 and 3151 (urea, s), ν(CO) 1645 (DMA, s), 1589 (urea, b); $\mu_{eff} = 5.34\ \mu_B$ (solid, 297 K).

Potassium {Tris[(*N*′-*tert*-butylureaylato)-*N*-ethyl]aminato(hydroxo)}cobaltate(II) ($K_2[Co^{II}H_3\mathbf{1}(OH)]$). $K_2[Co^{II}H_3\mathbf{1}(OH)]$ was synthesized following method B as described above for $K_2[Fe^{II}H_3\mathbf{1}(OH)]$. The salt was isolated as a magenta powder (63%). X-ray quality crystals (53%) were grown by vapor diffusion of diethyl ether into a DMA solution of $K_2[Co^{II}H_3\mathbf{1}(OH)]$. Anal. Calcd (found) for $K_2[Co^{II}H_3\mathbf{1}(OH)]\cdot 2DMA$, $C_{29}H_{61}CoK_2N_9O_6$: C, 45.30 (45.34); H, 7.92 (8.03); N, 16.28 (15.88). Spectroscopic and magnetic properties were identical to those reported for this complex when made by method A (vide supra).

Potassium {Tris[(*N*′-*tert*-butylureaylato)-*N*-ethyl]aminato(hydroxo)}zincate(II) ($K_2[Zn^{II}H_3\mathbf{1}(OH)]$). $K_2[Zn^{II}H_3\mathbf{1}(OH)]$ was synthesized following method B as described for $K_2[Fe^{II}H_3\mathbf{1}(OH)]$. The salt was isolated as a fine white powder (0.20 g, 64%) and washed four times with diethyl ether. X-ray quality crystals (0.12 g, 40%) were obtained by diffusing diethyl ether into a DMA solution of the complex. Anal. Calcd (found) for $K_2[Zn^{II}H_3\mathbf{1}(OH)]\cdot 2DMA$, $C_{29}H_{61}ZnK_2N_9O_6$: C, 45.31 (45.34); H, 7.94 (8.04); N, 16.40 (15.92). FTIR (Nujol, cm^{-1}): the $\nu(Zn^{II}O-H)$ was not observed, ν(NH) 3232 and 3154 (urea, s), ν(CO) 1645 (DMA, s), 1592 (urea, b).

(11) For a recent review on monomeric $Zn^{II}-OH$ complexes see: Parkin, G. *Chem. Commun.* **2000**, 1971−1985.
(12) (a) Harata, M.; Jitsukawa, K.; Masuda, H.; Einaga, H. *Chem. Lett.* **1995**, 61−62. (b) Wada, A.; Harata, M.; Hasegawa, K.; Jitsukawa, K.; Masuda, H.; Mukai, M.; Kitagawa, T.; Einaga, H. *Angew. Chem., Int. Ed.* **1998**, *37*, 798−799.
(13) Berreau, L. M.; Mahapatra, S.; Halfen, J. A.; Young, V. G., Jr.; Tolman, W. B. *Inorg. Chem.* **1996**, *35*, 6339−6342.
(14) Berreau, L. M.; Allred, R. A.; Makowski-Grzyska, M. M.; Arif, A. M. *Chem. Commun.* **2000**, 1423−1424.
(15) Other representative examples of H-bonding systems:[8] (a) Quinn, R.; Mercer-Smith, J.; Burstyn, J. N.; Valentine, J. S. *J. Am. Chem. Soc.* **1984**, *106*, 4136. (b) Wuenschell, G. E.; Tetreau, C.; Lavalette, D.; Reed, C. A. *J. Am. Chem. Soc.* **1992**, *114*, 3346−3355. (c) Collman, J. P.; Zhang, X.; Wong, K.; Brauman, J. I. *J. Am. Chem. Soc.* **1994**, *116*, 6245−6251. (d) Momenteau, M.; Reed, C. A. *Chem. Rev.* **1994**, *94*, 659−698. (e) Chang, C. K.; Liang, Y.; Avilés, G.; Peng, S.-M. *J. Am. Chem. Soc.* **1995**, *117*, 4191−4192. (f) Kickham, J. E.; Loeb, S. J.; Murphy, S. L. *J. Am. Chem. Soc.* **1993**, *115*, 7031−7032. (g) Rudkevich, D. M.; Verboom, W.; Brzozka, Z.; Palys, M. J.; Stauthamer, W. P. R. V.; Van Hummel, G. J.; Franken, S. M.; Harkema, S.; Engbersen, J. F. J.; Reinhoudt, D. N. *J. Am. Chem. Soc.* **1994**, *116*, 4341−4351. (h) Kitajima, N.; Komatsuzaki, H.; Hikichi, S.; Osawa, M.; Moro-oka, Y. *J. Am. Chem. Soc.* **1994**, *116*, 11596−11597. (i) Walton, P. H.; Raymond, K. N. *Inorg. Chim. Acta* **1994**, *240*, 593−601. (j) Yao, W.; Crabtree, R. H. *Inorg. Chem.* **1996**, *35*, 3007−3011.
(16) (a) Hammes, B. S.; Young, V. G., Jr.; Borovik, A. S. *Angew. Chem., Int. Ed.* **1999**, *38*, 666−669. (b) Shirin, Z.; Hammes, B. S.; Young, V. G., Jr.; Borovik, A. S. *J. Am. Chem. Soc.* **2000**, *122*, 1836−1837. (c) MacBeth, C. E.; Golombek, A. P.; Young, V. G., Jr.; Yang, C.; Kuczera, K.; Hendrich, M. P.; Borovik, A. S. *Science* **2000**, *289*, 938−941.

Synthesis of $M^{III}-OH$ Complexes. Potassium {Tris[(*N*′-*tert*-butylureaylato)-*N*-ethyl]aminato(hydroxo)}ferrate(III) (K[$Fe^{III}H_3$1**(OH)]).**[17] A solution of $K_2[FeH_3$**1**(OH)] (0.11 g, 0.18 mmol) in 5 mL of DMA was treated with dry O_2 ($T = 298$ K; $P = 0.99$ atm, $V = 4.4$ mL, 0.18 mmol), which caused an immediate color change from pale yellow to dark red. The mixture was stirred for 1 h and evacuated for 5 min. The resulting solution was filtered, and volatiles were removed under reduced pressure. The salt was crystallized by vapor diffusion of diethyl ether into a DMA solution of K[$Fe^{III}H_3$**1**(OH)] to afford a deep red microcrystalline product in 80% (0.089 g) yield. Anal. Calcd (found) for K[$Fe^{III}H_3$**1**(OH)]·2DMA, $C_{28}H_{61}FeKN_9O_6$: C, 47.92 (48.42); H, 8.28 (8.40); N, 17.41 (17.33). IR (Nujol, cm^{-1}): $\nu(^{16}OH)$ 3632, $\nu(^{18}OH)$ 3621, ν(NH) 3288 and 3181 (urea, b), ν(CO) 1645 (DMA, s), 1588 and 1547 (urea, s). $\lambda_{max/nm}$ (DMA, ϵ, M^{-1} cm^{-1}): 382 (1608); $\mu_{eff} = 5.99$ μ_B (solid, 297 K). The oxidation was also accomplished by using ferrocinium in place of dioxygen. The product was isolated in 68% yield.

Potassium {Tris[(*N*′-*tert*-butylureaylato)-*N*-ethyl]aminato](hydroxo)}cobaltate(III) (K_2[$Co^{III}H_3$1**(OH)]).**[16a] $K_2[Co^{III}H_3$**1**(OH)] was synthesized following the method described for K[$Fe^{III}H_3$**1**(OH)]. The salt was isolated as a red powder and crystallized by vapor diffusion of diethyl ether into a DMF solution of K[$Co^{III}H_3$**1**(OH)] (0.64 g, 47% yield). Anal. Calcd (found) for K[$Co^{III}H_3$**1**(OH)], $C_{21}H_{42}CoKN_7O_3$: C, 45.38 (44.93); H, 7.81 (7.86); N, 17.64 (17.24). IR (Nujol, cm^{-1}): ν(OH) 3616 (w), 3594 (w), ν(NH) 3366, 3251, 3161 (urea, m), ν(CO) 1599, 1581, 1522 (urea, s). UV/vis (DMF): 288 (ϵ, 6600), 389 (sh), 474 (ϵ, 3900), 793 (ϵ, 480); $\mu_{eff} = 3.28(6)$ μ_B (solid, 298 K). When ferrocinium was used as the oxidant, the product was isolated in 47% yield.

Physical Methods. Electronic spectra were recorded with a Cary 50 spectrophotometer. FTIR spectra were collected on a Mattson Genesis series FTIR instrument and are reported in wavenumbers. Room-temperature magnetic susceptibility measurements of solid samples were obtained using a MSB-1 magnetic susceptibility balance (Johnson Matthey). Diamagnetic corrections were taken from those reported by O'Connor.[18] X-band EPR spectra were collected using a Bruker EMX spectrometer equipped with an ER041XG microwave bridge. Spectra for all EPR active samples were collected using the following spectrometer settings: attenuation of 25 dB, microwave power of 0.638 mW, frequency of 9.48 GHz, sweep width of 5000 G, modulation amplitude of 31.99 G, gain of 3.56×10^{-3}, conversion time of 81.920 ms, time constant of 327.68 ms, and resolution of 1024 points. A quartz liquid nitrogen finger Dewar (Wilmad Glass) was used to record spectra at 77 K.

Cyclic voltammetric (CV) experiments were conducted using a BAS CV 50W (Bioanalytical Systems Inc., West Lafayette, IN) voltammetric analyzer following methods previously described.[19] Anhydrous DMF was obtained from Aldrich Chemical Co. and used without further purification. A ferrocinium/ferrocene couple was used to monitor the reference electrode (Ag/Ag^+) and was observed at 0.49 V with $\Delta E_p = 0.062$ V and $i_{pa}i_{pc}^{-1} = 0.98$ in DMF under ambient temperature. A glass carbon electrode was used as the working electrode. IR compensation was achieved before each CV was recorded. Potentials are reported vs the saturated calomel couple.

Crystallographic Structural Determination. All crystals were attached to a glass fiber under nitrogen and mounted on a Siemens SMART system for data collection at 173(2) K. An initial set of cell constants was calculated from reflections harvested from three sets of 20 frames. These initial sets of frames are oriented such that orthogonal wedges of reciprocal space were surveyed. For $K_2[Fe^{II}H_3$**1**(OH)]·4DMF, this produces orientation matrixes determined from 302 reflections. Final cell constants were calculated from a set of 7281 strong reflections from the actual data collection. For $K_2[Co^{II}H_3$**1**(OH)]·4DMF, this produces orientation matrixes determined from 294 reflections for the actual data collection. Final cell constants were calculated from 2046 strong reflections for the actual data collected after integration (SAINT 6.0.1, 1999). For $K_2[Zn^{II}H_3$**1**(OH)]·4DMF, this produces orientation matrixes determined from 303 reflections. Final cell constants were calculated from a set of 7284 strong reflections from the actual data collection. For K[$Co^{III}H_3$**1**(OH)], this produces orientation matrixes determined from 47 reflections. Final cell constants were calculated from a set of 4873 strong reflections from the actual data collection. See the appropriate tables for additional crystal and refinement information. The data collection technique used for these samples is generally known as a hemisphere collection. A randomly oriented region of reciprocal space is surveyed to the extent of 1.3 hemispheres to a resolution of 0.84 Å. Three major swaths of frames are collected with 0.30° steps in ω.

Structure Solution and Refinements. $K_2[Fe^{II}H_3$**1**(OH)]·4DMF crystallized in the space group $P2_1/n$, which was determined on the basis of systematic absences and intensity statistics. The structure was solved by direct methods. Several full-matrix least-squares/difference Fourier cycles were performed which located all non-hydrogen atoms. All non-hydrogen atoms were refined with anisotropic displacement parameters. All hydrogen atoms were placed in ideal positions and refined as riding atoms with relative isotropic displacement parameters. The unit cell was found to be primitive monoclinic with a and c axes nearly the same length. The β angle is 107.954(2)°. This unit cell can be transformed to a *C*-centered orthorhombic cell with twice the volume, but this appears to be coincidental. R_{int} for the corrected monoclinic cell is 0.054, while the *C*-centered orthorhrombic cell is 0.167. These results suggest that pseudomerohedral twinning is present. The twin components are in a 66:33 ratio by the 9 (row) [0 0 1/0 −1 0/1 0 0] twin law. In this case, it appears that reflections were not split appreciably. There were two independent molecules in the asymmetric unit denoted by "a" and "b". A pair of DMA molecules (out of a total of eight) is disordered positionally over a pair of sites (J/K/J′/K′). Some of the DMA groups are refined as disordered groups where the C═N parts cross (G/G′/I/I′). FLAT and SAME restraints were applied along with the appropriate displacement restraints. All atoms are refined with anisotropic displacements, and 924 restraints were used in total. The hydroxo hydrogen was refined torsionally. The NH protons were placed ideally. Two of the eight solvate molecules are corner-to-corner disordered. Those that require two partial molecules have the same atoms in common. EADP and EXYZ constraints were used where appropriate. All were refined SAME/FLAT/DELU restraints. A total of 641 constraints were used. No additional symmetry was found.

$K_2[Co^{II}H_3$**1**(OH)]·4DMF was solved in a manner similar to $K_2[Fe^{II}H_3$**1**(OH)]·4DMF. $K_2[Zn^{II}H_3$**1**(OH)]·4DMF was similarly solved; the twin components in this structure are in a 69:31 ratio.

For K[$Co^{III}H_3$**1**(OH)], the space group $P\bar{1}$ was determined on the basis of the systematic absences and intensity statistics. A successful direct-methods solution was calculated which provided most non-hydrogen atoms from the E-map. Several full-matrix least-squares/difference Fourier cycles were performed which located the remainder of the non-hydrogen atoms. All non-hydrogen atoms were refined with anisotropic displacement parameters and refined as riding atoms with relative isotropic displacement parameters. For the anion, $[Co^{III}H_3$**1**(OH)]$^-$, the ureayl arm containing O2 and N3 exhibited a high degree of anisotropic displacement. Both O2 and N3 exhibit a librational motion by rotation about an axis that is approximately parallel to an axis through N2 and C4. The methyl groups attached to C4 also are disordered. All atoms beyond C3 were split into two fragments and refined with restraints. The refinement led to a 0.48:0.52 ratio in occupancy. Fifty-two SHELXTL, SAME, and FLAT restraints were applied to atom groups of a similar nature.

Results and Discussion

Syntheses. Two different synthetic routes, denoted methods A and B, have been used to isolate monomeric $M^{II}-OH$ complexes (Scheme 1). Method A utilizes 3 equiv of base to triply deprotonate H_6**1** to form $[H_3$**1**$]^{3-}$, which then binds a metal ion to afford $[M^{II}H_3$**1**$]^{1-}$. Without isolation, the $[M^{II}H_3$**1**$]^{1-}$ complexes are treated with 2 equiv of H_2O to form metal complexes with a terminal hydroxo ligand. This method was

(17) This complex can also be made directly from dioxygen; see ref 16c.
(18) O'Connor, C. J. *Prog. Inorg. Chem.* **1992**, *29*, 203−283.
(19) Ray, M.; Hammes, B. S.; Yap, G. P. A.; Rheingold, A. H.; Liable-Sands, L.; Borovik, A. S. *Inorg. Chem.* **1998**, *37*, 1527−1532.

Scheme 1[a]

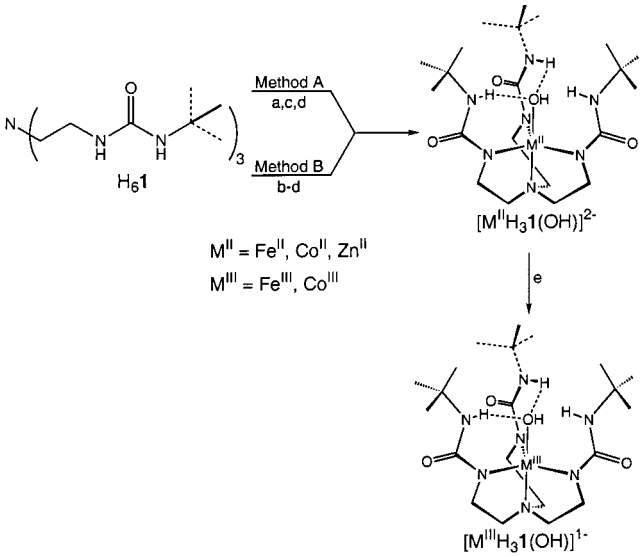

[a] Conditions: (a) 3 equiv KH, DMA, Ar, RT; (b) 4 equiv KH, DMA, Ar, RT; (c) $M^{II}(OAc)_2$, DMA, Ar, RT; (d) H_2O, RT; (e) [O], DMA, RT.

reported previously for the formation of $[Co^{II}H_3\mathbf{1}(OH)]^{2-}$, which was isolated in 40% yield.[16a,20] A possible explanation for this low yield is that $[H_3\mathbf{1}]^{3-}$ is protonated in half of the complexes when water is converted to hydroxide. Protonation most likely occurs at the apical amine, which is the most basic site in the complex. This would result in the complexes being relatively unstable and hinder their isolation. This hypothesis has also been proposed for the less than 50% yield observed for $[Co(np_3)(OH)]^+$ (np_3, tris(2-diphenylphosphinoethyl) amine), another monomeric Co^{II}−OH complex containing a tripodal ligand with an apical amine donor.[9]

M^{II}−OH complexes made by method B routinely produced higher yields than those obtained by method A. For example, greater than 50% yield of crystalline $[Co^{II}H_3\mathbf{1}(OH)]^{2-}$ is achieved when the complex is made by method B. This synthetic method differs from method A by employing 4 equiv of base. The extra equivalent of base in method B deprotonates an α′-N−H group on one of the tripodal arms in $H_6\mathbf{1}$ to give $[H_2\mathbf{1}]^{4-}$. This affords complexes, $[M^{II}H_2\mathbf{1}]^{2-}$, which have a general base (the N^- group) within the cavity. Modeling studies (CAChe) show that an α′-N^- can be positioned within the cavity to accept the proton produced when hydroxide is formed from water. Proton transfers would yield the desired $[M^{II}H_3\mathbf{1}(OH)]^{2-}$ complexes, in which all three α′-N−H groups are directed into the cavity and available for H-bonding to the coordinated hydroxo ligand (Figure 1). Method B thus avoids protonation of other sites on the tripodal ligands that would produce less stable complexes.

The improved yield observed by method B is attributed to the presence of an α′-N^- group within the cavity. Further support is provided by the synthesis of $[Co^{II}H_3\mathbf{1}(OH)]^{2-}$ using the method outlined in Scheme 2. The initial synthetic steps follow those of method A: $H_6\mathbf{1}$ is deprotonated with 3 equiv of KH and the resulting mixture is treated with $Co(OAc)_2$. The reaction mixture is filtered to remove 2 equiv of KOAc, which is insoluble in DMA. The filtrate containing the metal complex is then treated with 1 equiv of KH. After gas evolution ceases, 1 equiv of H_2O is added, and $[Co^{II}H_3\mathbf{1}(OH)]^{2-}$ is isolated as a crystalline solid in 60% yield.

(20) Attempts to synthesize $[Fe^{II}H_3\mathbf{1}(OH)]^{2-}$ and $[Zn^{II}H_3\mathbf{1}(OH)]^{2-}$ by method A were unsuccessful. Only insoluble solids were obtained.

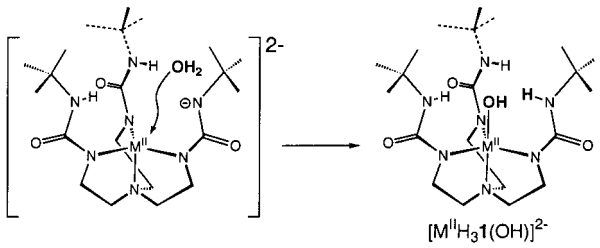

Figure 1. Proposed role of the deprotonated α′-N^- in the formation of the M^{II}−OH complexes.

Scheme 2[a]

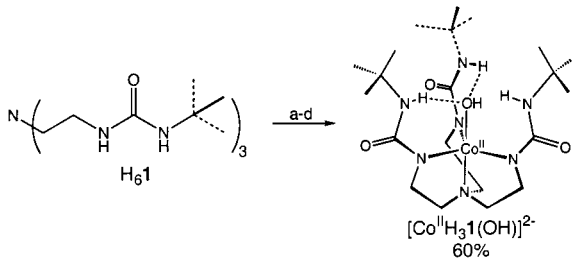

[a] Conditions: (a) 3 equiv KH, DMA, Ar, RT; (b) $Co(OAc)_2$, DMA, Ar, RT; (c) 1 equiv KH, DMA, Ar, RT; (d) H_2O, RT.

Treating $[Co^{II}H_3\mathbf{1}(OH)]^{2-}$ and $[Fe^{II}H_3\mathbf{1}(OH)]^{2-}$ with an oxidant (O_2 or ferrocinium) results in formation of the corresponding M^{III}−OH complexes. Water is the source of the hydroxo ligand in these oxidized products. This was confirmed for $[Co^{III}H_3\mathbf{1}(OH)]^{1-}$ by labeling studies, in which no change in the frequency of the O−H stretch was observed when $^{18}O_2$ was used. However, ^{18}O was incorporated into $[Co^{III}H_3\mathbf{1}(OH)]^{1-}$ when $H_2{}^{18}O$ was employed in the reaction: $\nu(^{16}OH) = 3616$, 3594 cm^{-1}, $\nu(^{18}OH) = 3606$, 3582 cm^{-1}, $\nu(^{16}OH)/\nu(^{18}OH) = 1.003$, 1.003; calcd = 1.003. Analogous findings were also obtained for $[Fe^{III}H_3\mathbf{1}(OH)]^{1-}$.

All the M−OH complexes are stable in the solid state under anhydrous and anaerobic conditions. In solution, the $Fe^{II/III}$−OH and $Co^{II/III}$−OH complexes are stable over a period of days. In contrast, the $[Zn^{II}H_3\mathbf{1}(OH)]^{2-}$ is far less stable in solvents such as $CDCl_3$ and DMSO-d_6, which has prevented full characterization of this complex in solution. Similar instability was observed for previously reported zinc complexes with terminal hydroxo ligands.[21] Studies into understanding this solution instability are ongoing.

Solid-State Structures of the Complexes: General Lattice Properties. Single-crystal X-ray diffraction studies were conducted on $K_2[Co^{II}H_3\mathbf{1}(OH)]\cdot 4DMA$, $K_2[Fe^{II}H_3\mathbf{1}(OH)]\cdot 4DMA$, $K_2[Zn^{II}H_3\mathbf{1}(OH)]\cdot 4DMA$, and $K[Co^{III}H_3\mathbf{1}(OH)]$. Crystal, data collection, and refinement parameters are given in Table 1, and selected distances and angles are presented in Table 2. Additional structural parameters and figures are provided in Supporting Information.

Single crystals of $K[Co^{III}H_3\mathbf{1}(OH)]$ belong to the triclinic space group $P\bar{1}$. This salt crystallized without any additional solvent. The individual anions are linked by K^+ ions that bridge between the urea oxygens of the $[H_3\mathbf{1}]^{3-}$ ligands. This bridging motif is shown in Figure 2. Each potassium ion is four-coordinate with an average K−O distance of 2.617(4) Å.

$K_2[Co^{II}H_3\mathbf{1}(OH)]\cdot 4DMA$, $K_2[Fe^{II}H_3\mathbf{1}(OH)]\cdot 4DMA$, and $K_2[Zn^{II}H_3\mathbf{1}(OH)]\cdot 4DMA$ crystallize in the monoclinic space group $P2_1/n$ and have nearly identical lattice parameters (Table 1). Each salt crystallized with two independent, but structurally

(21) Alsfasser, R.; Trofimenko, S.; Looney, A.; Parkin, G.; Vahrenkamp, H. *Inorg. Chem.* **1991**, *30*, 4098−4100.

Table 1. Crystallographic Data for $[Fe^{II}H_3\mathbf{1}(OH)]^{2-}$, $[Co^{II}H_3\mathbf{1}(OH)]^{2-}$, $[Zn^{II}H_3\mathbf{1}(OH)]^{2-}$, and $[Co^{III}H_3\mathbf{1}(OH)]^{1-}$

complex	$K_2[Fe(H_3\mathbf{1})(OH)]\cdot 4DMA$	$K_2[Co(H_3\mathbf{1})(OH)]\cdot 4DMA$	$K_2[Zn(H_3\mathbf{1})(OH)]\cdot 4DMA$	$K[Co(H_3\mathbf{1})(OH)]$
molecular formula	$C_{74}H_{158}Fe_2K_4N_{22}O_{16}$	$C_{74}H_{158}Co_2K_4N_{22}O_{16}$	$C_{74}H_{158}K_4N_{22}O_{16}Zn_2$	$C_{21}H_{43}CoKN_7O_4$
fw	1880.3	1886.48	1899.4	555.65
T (°C)	−100(2)	−100(2)	−100(2)	−100(2)
space group	$P2_1/n$	$P2_1/n$	$P2_1/n$	$P\bar{1}$
a (Å)	30.663(3)	30.662(7)	30.675(3)	10.7773(3)
b (Å)	11.4858(11)	11.504(2)	11.5035(5)	11.3017(3)
c (Å)	30.708(3)	30.688(6)	30.727(3)	11.7250(2)
α (deg)	90	90	90	94.319(1)
β (deg)	106.096(2)	106.615(4)	106.4150(1)	95.146(1)
γ (deg)	90	90	90	98.003(1)
Z	4	4	4	2
V (Å^3)	10 391(2)	10 373(4)	10 400.7(12)	1402.94(6)
δ_{calcd} (mg/m^3)	1.202	1.208	1.213	1.315
R^a	0.0531	0.0546	0.0478	0.0463
$R_w{}^b$	0.0629	0.0714	0.0701	0.0680
GOF^c	1.050	1.047	0.955	0.989

[a] $R = [\sum|\Delta F|/\sum|F_o|]$. [b] $R_w = [\sum w(\Delta F)^2/\sum wF_o^2]$. [c] Goodness of fit on F^2.

Table 2. Selected Bond Distances and Angles for $[Zn^{II}H_3\mathbf{1}(OH)]^{2-}$, $[Fe^{II}H_3\mathbf{1}(OH)]^{2-}$, $[Co^{II}H_3\mathbf{1}(OH)]^{2-}$, and $[Co^{III}H_3\mathbf{1}(OH)]^{1-}$ [a]

	$[Zn^{II}H_3\mathbf{1}(OH)]^{2-}$	$[Fe^{II}H_3\mathbf{1}(OH)]^{2-}$	$[Co^{II}H_3\mathbf{1}(OH)]^{2-}$	$[Co^{III}H_3\mathbf{1}(OH)]^{1-}$
		Distance (Å)		
M1A−N1A	2.274(3)	2.254(3)	2.216(4)	1.945(3)
M1B−N1B	2.285(4)	2.253(3)	2.212(4)	
M1A−N2A	2.052(4)	2.084(4)	2.046(4)	1.957(3)
M1B−N2B	2.052(4)	2.086(4)	2.050(4)	
M1A−N4A	2.093(4)	2.110(3)	2.075(4)	1.974(3)
M1B−N4B	2.089(3)	2.104(4)	2.073(4)	
M1A−N6A	2.106(3)	2.112(4)	2.079(4)	1.939(3)
M1B−N6B	2.098(3)	2.121(4)	2.085(4)	
M1A−O1A	2.029(3)	2.051(3)	2.051(3)	1.894(2)
M1B−O1B	2.019(3)	2.044(3)	2.053(3)	
O1A···N3A	2.793(6)	2.812(6)	2.802(6)	2.799(13)[b]
O1B···N3B	2.858(6)	2.868(6)	2.838(6)	
O1A···N5A	2.820(5)	2.854(5)	2.782(5)	2.748(4)
O1B···N5B	2.779(5)	2.821(5)	2.774(5)	
O1A···N7A	2.838(5)	2.875(6)	2.829(5)	2.680(4)
O1B···N7B	2.800(5)	2.842(5)	2.773(5)	
		Angle (deg)		
N1A−M1A−O1A	179.25(14)	179.81(13)	179.31(15)	175.94(11)
N1B−M1B−O1B	178.26(14)	178.97(14)	178.34(14)	
N2A−M1A−N4A	118.09(14)	118.98(14)	118.40(15)	108.16(11)
N2B−M1B−N4B	123.62(14)	125.85(14)	123.78(15)	
N2A−M1A−N6A	124.7(2)	125.4(2)	125.04(16)	132.35(11)
N2B−M1B−N6B	119.13(14)	118.58(14)	119.60(14)	
N4A−M1A−N6A	107.34(14)	105.65(14)	108.12(15)	116.36(11)
N4B−M1B−N6B	107.51(14)	105.70(14)	108.25(15)	
N1A−M1A−N2A	79.6(2)	79.71(14)	80.17(15)	82.80(11)
N1B−M1B−N2B	79.90(14)	80.36(14)	80.74(15)	
N1A−M1A−N4A	79.66(13)	79.43(13)	80.66(14)	84.82(1)
N1B−M1B−N4B	79.25(13)	79.06(13)	79.93(14)	
N1A−M1A−N6A	79.33(13)	79.25(13)	80.16(14)	85.05(11)
N1B−M1B−N6B	79.50(13)	79.03(13)	80.31(14)	

[a] There are two independent anions in the asymmetric unit for the $[M^{II}H_3\mathbf{1}(OH)]^{2-}$ complexes. Metric parameters for both are reported. The standard errors in the metrical parameters are slightly underestimated because of crystallographic twinning. [b] The urea arm containing N3 is disordered over two positions. The distance reported is for one fragment.

similar, anions in the asymmetric unit (referred to as "a" and "b"). The lattices of these salts also have potassium ions bridged between the anions. This is illustrated in Figure 3A for $K_2[Zn^{II}H_3\mathbf{1}(OH)]\cdot 4DMA$. The bridging potassium ions have tetrahedral coordinate geometry. Three coordinate sites on K^+ are occupied by urea oxygens of the $[H_3\mathbf{1}]^{3-}$ ligand with an average $K-O_{urea}$ distance of 2.853 Å. The remaining site is filled by carbonyl oxygen of a DMA solvate molecule. This network of anions and cations form pleated sheets. A second, nonbridging, potassium ion also interacts with each anion. This K^+ is positioned in the crevice between two of the urea arms of $[H_3\mathbf{1}]^{3-}$. For $[Zn^{II}H_3\mathbf{1b}(OH)]^{2-}$, which is shown in Figure 3B, average $K1-N_{urea}$ and $K1-C_{urea}$ distances of 2.963 and 3.067 Å, respectively, are observed. Two carbonyl oxygens, O1G and O1H, from DMA complete the coordination sphere around the potassium ion where the average $K1-O_{DMA}$ distance is 2.632 Å. K1 is 3.833 Å from O1B, the hydroxo oxygen bonded to the zinc ion. The bonding around the potassium ions in $K_2[Zn^{II}H_3\mathbf{1}(OH)]\cdot 4DMA$ is nearly identical to that found in $K_2[Co^{II}H_3\mathbf{1}(OH)]\cdot 4DMA$ and $K_2[Fe^{II}H_3\mathbf{1}(OH)]\cdot 4DMA$.

Molecular Structures of $[M^{II}H_3\mathbf{1}(OH)]^{2-}$. The complexes $[Zn^{II}H_3\mathbf{1}(OH)]^{2-}$, $[Co^{II}H_3\mathbf{1}(OH)]^{2-}$, and $[Fe^{II}H_3\mathbf{1}(OH)]^{2-}$ also have similar molecular structures. This structure is illustrated by the thermal ellipsoid diagram of $[Zn^{II}H_3\mathbf{1}(OH)]^{2-}$ in Figure 4A. Each complex has a trigonal bipyramidal arrangement of donor atoms around the metal ion. The trigonal plane is defined

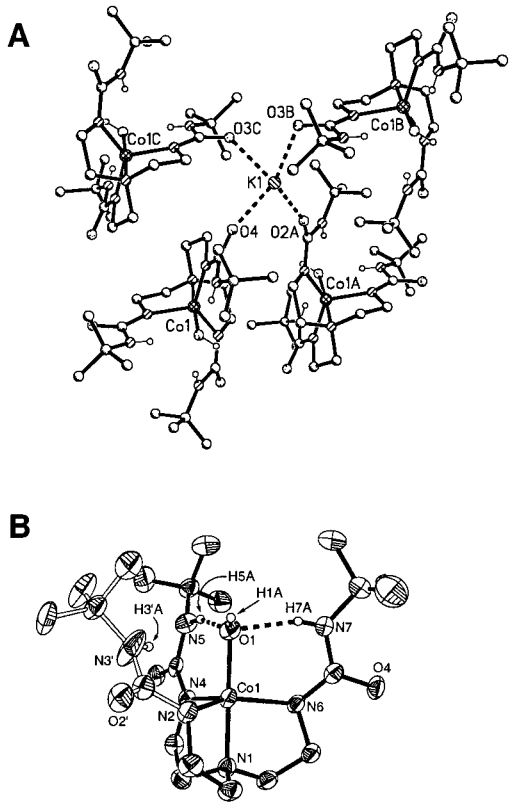

Figure 2. A view of the crystal lattice of K[$Co^{III}H_3$**1**(OH)] showing the cation−anion interactions (A) and a thermal ellipsoid diagram of [$Co^{III}H_3$**1b**(OH)]$^{1-}$ (B). The ellipsoids are drawn at the 50% probability level, and only the urea and hydroxo hydrogens are shown for clarity. Only one of the disordered fragments for the arm containing N2 is shown.

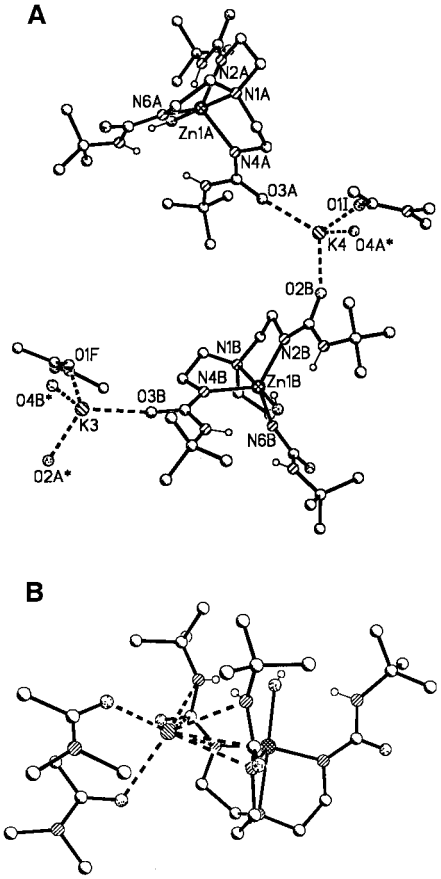

Figure 3. Two views for a portion of the crystal lattice of K_2-[$Zn^{II}H_3$**1**(OH)]·4DMA illustrating the cation−anion interactions: (A) the K^+−carbonyl oxygen interactions; (B) positioning of a K^+ ion in the crevice between two of the cavity arms.

by the three deprotonated urea nitrogens, N2, N4, and N6, of the [H_3**1**]$^{3-}$ ligand. The apical nitrogen, N1, is positioned trans to the O1 of the hydroxo ligand: all the N1−M−O1 angles are greater than 178°. The remaining components of the urea groups form a hydrogen-bond cavity that surrounds the M−OH unit. The structures of the cavities in the three complexes are nearly identical. This is shown in Figure 4B, where an overlay of the molecular structures for the three anions is displayed. The urea N−H groups are positioned inside the cavity with N···O1 distances of <2.9 Å. Two of these groups, N3−H and N5−H, are directed toward the hydroxo O1, which is indicative of intramolecular hydrogen bonding (Table 2). In anion a of each structure, refinement of the urea and hydroxo hydrogens did not accurately determine their positions. This problem did not occur in anion b. Details of the molecular structures of [$M^{II}H_3$**1**(OH)]$^{2-}$ and their relationship to previously reported complexes are discussed in the following paragraphs.

[$Zn^{II}H_3$1(OH)]$^{2-}$. The prevalence of Zn−OH units in the active of sites of hydrolytic enzymes has sparked efforts to make synthetic complexes containing this moiety.[10,22] Only three structures of monomeric Zn−OH complexes have been reported, all of which are four-coordinate.[22,23] Tris(pyrazolyl)hydroborato ($Tp^{R,R'}$) or tris[2-(1-isopropyl-4-*tert*-butylimidazolyl)] phosphine ($Pim^{t-Bu,i}Pr$) ligands complete the coordination sphere around the zinc ion. Zinc−oxygen bond distances of ∼1.850 Å are observed in [Zn($Tp^{t-Bu,Me}$)(OH)] and [Zn($Tp^{Cum,Me}$)(OH)], while in [Zn($Pim^{t-Bu,i}Pr$)(OH)]$^+$, the distance is 1.860(5) Å (Table 3).[24] Note that in these published complexes, bulky substituents are essential for the isolation of monomeric species; similar structural requirements are needed for the [$M^{II}H_3$**1**(OH)]$^{2-}$ complexes presented in this work.[25]

The two anions of [$Zn^{II}H_3$**1**(OH)]$^{2-}$ have significantly longer Zn−O bond lengths compared to those in the previously published complexes. [$Zn^{II}H_3$**1a**(OH)]$^{2-}$ has a Zn−O bond distance of 2.029(3) Å, while that in [$Zn^{II}H_3$**1b**(OH)]$^{2-}$ is 2.019(3) Å. A possible explanation for the different bond distances is that the unique microenvironment around the zinc−hydroxo unit in [$Zn^{II}H_3$**1**(OH)]$^{2-}$ causes a lengthening of the Zn−O bond. The presence of two intramolecular H-bonds (Zn−O···H−N) in [$Zn^{II}H_3$**1**(OH)]$^{2-}$ partially removes electron density from the hydroxo ligand. This would in turn produce a longer Zn−O bond distance than those observed in systems where H-bonds to the hydroxo oxygen are absent. Support for this hypothesis comes from the structural properties in the active site of the zinc-containing enzyme carbonic anhydrase II (CAII).[26] Figure 5 shows a portion of the active site in CAII, obtained from X-ray diffraction studies (1.54 Å resolution) of crystals isolated at pH = 7.8. The Zn−O(H) distance of 2.05(2) Å in CAII is less than 0.03 Å longer than that in [$Zn^{II}H_3$**1**(OH)]$^{2-}$.

(22) Kimura, E. *Acc. Chem. Res.* **2001**, *34*, 171−179.
(23) Ruf, M.; Vahrenkamp, H. *Inorg. Chem.* **1996**, *35*, 6571−6578.
(24) Kimblin, C.; Allen, W. E.; Parkin, G. *J. Chem. Soc., Chem. Commun.* **1995**, 1813−1815.
(25) Additional studies on monomeric Zn^{II}−OH complexes: (a) Looney, A.; Han, R.; McNeill, K.; Parkin, G. *J. Am. Chem. Soc.* **1993**, *115*, 4690−4697. (b) Kitajima, N.; Hikichi, S.; Tanaka, M.; Moro-oka, Y. *J. Am. Chem. Soc.* **1993**, *115*, 5496−5508.
(26) Håkansson, K.; Carlsson, M.; Svensson, L. A.; Liljas, A. *J. Mol. Biol.* **1992**, *227*, 1192−1204.

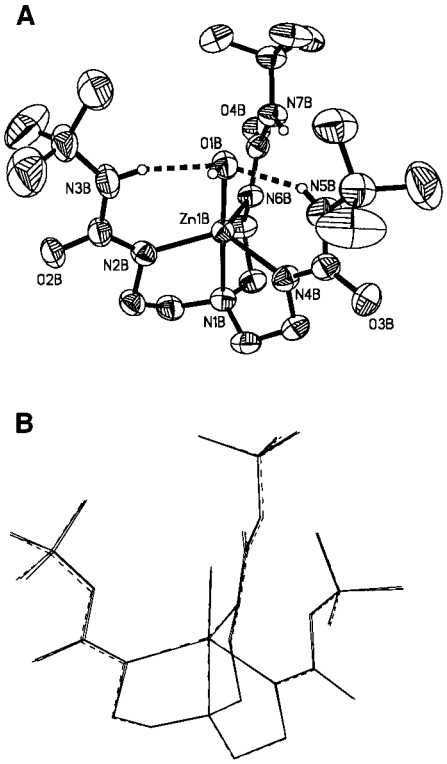

Figure 4. Thermal ellipsoid diagram of $[Zn^{II}H_3\mathbf{1b}(OH)]^{2-}$ (A) and overlay of the molecular structures of $[Zn^{II}H_3\mathbf{1b}(OH)]^{2-}$, $[Co^{II}H_3\mathbf{1b}(OH)]^{2-}$, and $[Fe^{II}H_3\mathbf{1b}(OH)]^{2-}$ (B). The ellipsoids are drawn at the 50% probability level, and only the urea and hydroxo hydrogens are shown for clarity.

Table 3. Comparison of $M^{II}-OH$ Bond Distances

complex	d(M−O) (Å)	ref
$[Zn^{II}H_3\mathbf{1}(OH)]^{2-}$	2.024(2)[a]	this work
$[Zn(Tp^{t-Bu,Me})(OH)]$	1.850(8)	22
$[Zn(Tp^{Cum,Me})(OH)]$	1.847(4)	23
$[Zn(Pim^{t-Bu,iPr})(OH)]^{+}$	1.860(5)	24
$[Zn([12]aneN_3)(OH)]_3^{3+}$	1.944(5)	27
[Zn(OH)]CAII	2.05(2)	26
$[Fe^{II}H_3\mathbf{1}(OH)]^{2-}$	2.048(3)[a]	this work
$[Fe(Tp^{t-Bu,iPr})(OH)]$	1.830(8)	6
$[Fe(Tp^{iPr,iPr})(\mu-OH)]_2$	2.016(9); 2.04(1)	28
$[Co^{II}H_3\mathbf{1}(OH)]^{2-}$	2.052(3)[a]	this work
$[Co(pp_3)(OH)]^{+}$	1.873(7)	9

[a] Reported as average values for the two anions in the asymmetric unit.

The Zn−OH unit in CAII, similar to the microenvironment in $[Zn^{II}H_3\mathbf{1}(OH)]^{2-}$, is surrounded by groups that can participate in H-bonding (Figure 5). Two water molecules, W318 and W338, are positioned close to the OH group, within distances consistent with H-bonds: the O-263···O-318 separation is 2.79 Å and O-263···O-338 is 2.60 Å. In addition, a H-bond between the Zn−OH and HO−Thr-199 is present (O-292···O-199, 2.83 Å). In this interaction, the Zn−OH unit serves as the H-bond donor (Zn−OH···O(H)−Thr-199). Finally, the solid-state structure of $[Zn([12]aneN_3)(OH)]_3^{3+}$ ([12]aneN$_3$, 1,5,9-triazacyclododecane) also contains Zn−OH units which are connect by a complex network of H-bonds within each trimer.[27] Zinc−oxygen distances of 1.944(5) Å are found for $[Zn([12]aneN_3)(OH)]_3^{3+}$, 0.080 Å shorter than that found in $[Zn^{II}H_3\mathbf{1}(OH)]^{2-}$.

$[Fe^{II}H_3\mathbf{1}(OH)]^{2-}$. Iron−oxygen bond distances of 2.051(3) and 2.044(3) Å are present in $[Fe^{II}H_3\mathbf{1a}(OH)]^{2-}$ and $[Fe^{II}H_3\mathbf{1b}(OH)]^{2-}$, respectively. These bond lengths are longer than the Zn−O distances in $[Zn^{II}H_3\mathbf{1}(OH)]^{2-}$ by an average of 0.024 Å. The metal−apical nitrogen (M−N1) distances in the iron and zinc complexes also differ slightly. In $[Zn^{II}H_3\mathbf{1}(OH)]^{2-}$, the average Zn−N1 length is 2.280(3) Å, while in $[Fe^{II}H_3\mathbf{1}(OH)]^{2-}$, the average Fe−N1 distance is longer at 2.254(2) Å.

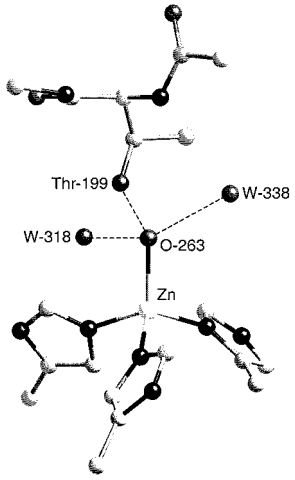

Figure 5. The active site of carbonic anhydrase II showing the H-bonds to the Zn−OH unit. The heavy atom distances are as follows: O-263···O-318, 2.79(2) Å; O-263···O-338, 2.60(2) Å, and O-292···O-199, 2.83(2) Å. Figure is adapted from ref 25.

Monomeric Fe^{II} complexes with terminal hydroxo ligands are rare. We are aware of only one other example, the four-coordinate $[Fe^{II}(Tp^{t-Bu,i}Pr)(OH)]$ complex of Hikichi and Moro-oka.[6] The Fe−O bond of 1.830(8) Å in this complex is significantly shorter than that found in $[Fe^{II}H_3\mathbf{1}(OH)]^{2-}$. Note that this is similar to the findings for the related Zn^{II} complexes (infra supra). In fact, the Fe−O distances for the two anions of $[Fe^{II}H_3\mathbf{1}(OH)]^{2-}$ are comparable to the 2.016(9) and 2.04(1) Å distances reported for Fe−O bonds in $[Fe(Tp^{i}Pr,^{i}Pr)(\mu-OH)]_2$, a bis-$\mu$-hydroxo bridged dimer.[28]

$[Co^{II}H_3\mathbf{1}(OH)]^{2-}$. $[Co^{II}H_3\mathbf{1a}(OH)]^{2-}$ and $[Co^{II}H_3\mathbf{1b}(OH)]^{2-}$ have Co1−O1 bond lengths of 2.053(3) and 2.051(3) Å. The closest examples to $[CoH_3\mathbf{1}(OH)]^{2-}$ are the monomeric, five-coordinate cobalt−hydroxo complexes of Orlandini and Sacconi.[9] The molecular structure of only $[Co^{II}(pp_3)(OH)]^{+}$ (pp_3, $P[CH_2CH_2P(Ph)_2]_3$) has been reported. This previously reported complex has a distorted square pyramidal coordination geometry, with the terminal hydroxo ligand in the basal plane. A Co−O(H) bond length of 1.873(7) Å is found in $[Co^{II}pp_3(OH)]^{+}$. However, $[Co^{II}pp_3(OH)]^{+}$ is low-spin, which prevents a direct comparison to the metrical parameters for the high-spin complex $[Co^{II}H_3\mathbf{1}(OH)]^{2-}$. It is interesting to note that in the crystal lattice of $[Co^{II}pp_3(OH)]BF_4\cdot C_2H_5OH$, the hydroxo ligand in $[Co^{II}pp_3(OH)]^{+}$ forms an intermolecular H-bond with the ethanol solvate (HO···O(H)Et, 2.61 Å). Details into this H-bonding interaction and its affect on the Co−O bond distance were not described.

Molecular Structure of $[Co^{III}H_3\mathbf{1}(OH)]^{1-}$. This Co^{III} complex also has a trigonal bipyramidal coordination geometry, with the terminal hydroxo ligand being trans to the apical amine nitrogen of the $[H_3\mathbf{1}]^{3-}$ ligand. In $[Co^{III}H_3\mathbf{1}(OH)]^{1-}$, the Co1−O1 and Co1−N1 distances are 1.894(2) and 1.945(3) Å and the average Co1−N_{urea} bond length is 1.957(2) Å (Figure 2B and Table 2). These reductions in bond lengths, compared to those found in $[Co^{II}H_3\mathbf{1}(OH)]^{2-}$, are consistent with the observed oxidation and spin-state changes at the cobalt center from $S =$

(27) Kimura, E.; Shiota, T.; Koike, T.; Shiro, M.; Kodama, M. *J. Am. Chem. Soc.* **1990**, *112*, 5805−5811.

(28) Kitajima, N.; Tamura, N.; Tanaka, M.; Moro-oka, Y. *Inorg. Chem.* **1992**, *31*, 3342−3343.

2 to $S = 1$ (vide infra). The N2−Co1−N6 angle of 132.35(11)° in $[Co^{III}H_3\mathbf{1}(OH)]^{1-}$ is larger than what is predicted for trigonal bipyramidal complexes. The lengthening of this angle is caused by the placement of the hydroxo O1−H1 vector between the urea arms containing N2 and N6. An increase in one of the trigonal angles is also seen in the M^{II}−OH complexes, but the effect is not as large as that in $[Co^{III}H_3\mathbf{1}(OH)]^{1-}$ (Table 2).

$[Co(terpy)(\eta^2\text{-}CO_3)(OH)]\cdot 4H_2O$ (terpy, 2,2′:6′,2″-terpyridine) is the only other monomeric Co^{III}−OH complex for which the structure is known.[9] This six-coordinate complex has a Co−O(H) distance of 1.894(10) Å, the same as in $[Co^{III}H_3\mathbf{1}(OH)]^{1-}$. The hydroxo ligand in $[Co(terpy)(\eta^2\text{-}CO_3)(OH)]$ is involved in three intermolecular H-bonds within the crystal lattice: two arise from the hydroxo oxygen accepting H-bonds from two water solvates, while the remaining one involves the hydroxo ligand donating an H-bond to a third water molecule. The presence of these H-bonds in $[Co(terpy)(\eta^2\text{-}CO_3)(OH)]$ is similar to what is observed in $[Co^{III}H_3\mathbf{1}(OH)]^{1-}$, although in the latter complex the H-bonds are intramolecular. Nevertheless, this may account for the same Co−O(H) bond distances observed in the two complexes. Other Co^{III}−OH complexes are polynuclear with bridging hydroxo ligands in the solid state.[29] These include the Werner-type complexes $[CoL_4(H_2O)(OH)]^{2-}$, which are dimeric in the solid state with bridging $H_3O_2^-$ ligands.[30]

Physical and Electrochemical Properties. The Co−OH and Fe−OH complexes are high-spin. $[Co^{II}H_3\mathbf{1}(OH)]^{2-}$ has a room-temperature magnetic moment of 4.49 μ_B and a broad X-band EPR signal centered at $g = 3.87$; both data support the assignment of an $S = {}^3/_2$ ground state. $[Co^{III}H_3\mathbf{1}(OH)]^{1-}$ is also paramagnetic ($S = 1$) with a room temperature μ_{eff} of 3.28(6) μ_B.[31] A ground state of $S = 1$ for $[Co^{III}H_3\mathbf{1}(OH)]^{1-}$ is consistent with the trigonal bipyramidal geometry around the cobalt center. There are few examples of paramagnetic Co^{III} species,[32] the norm being complexes that are diamagnetic. The formation of the more common six-coordinate complexes is prevented in $[Co^{III}H_3\mathbf{1}(OH)]^{1-}$ by the H-bond cavity of $[H_3\mathbf{1}]^{3-}$, which shields the metal center and prohibits additional binding of external ligands.

$[Fe^{II}H_3\mathbf{1}(OH)]^{2-}$ has a $S = 2$ ground state with a room-temperature magnetic moment of 5.34 μ_B. The high-spin $[Fe^{III}H_3\mathbf{1}(OH)]^{1-}$ complex has a μ_{eff} of 5.99 μ_B at room temperature. The 4.2 K X-band EPR spectrum has features at $g = 8.9$, 1.4 and $g = 5.3$, 3.4, with an E/D of 0.17. The anisotropy associated with the spectrum is consistent with distortions in the ligand field geometry surrounding the Fe^{III} center. Such distortions were observed in the solid-state molecular structure of $[Co^{III}H_3\mathbf{1}(OH)]^{1-}$, a complex that has a similar molecular composition as $[Fe^{III}H_3\mathbf{1}(OH)]^{1-}$ (vide supra).

The cyclic voltammograms (CV) for $[Co^{II}H_3\mathbf{1}(OH)]^{2-}$ and $[Fe^{II}H_3\mathbf{1}(OH)]^{2-}$ are shown in Figure 6. Both complexes have reversible one-electron redox couples with potentials of < -0.50 V. For $[Co^{II}H_3\mathbf{1}(OH)]^{2-}$, this redox process occurs at $E_{1/2} = -0.74$ V vs SCE with $i_{pa}i_{pc}^{-1} = 0.97$ and $\Delta E_P = 0.14$ V. A more negative redox potential is exhibited by $[Fe^{II}H_3\mathbf{1}(OH)]^{2-}$:

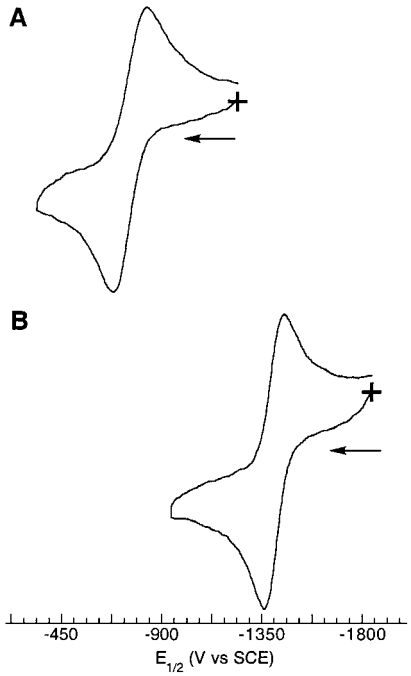

Figure 6. Cyclic voltammograms of $[Co^{II}H_3\mathbf{1}(OH)]^{2-}$ (A) and $[Fe^{II}H_3\mathbf{1}(OH)]^{2-}$ (B) recorded at a scan rate of 0.100 V s^{-1}.

$E_{1/2} = -1.40$ V vs SCE with $i_{pa}i_{pc}^{-1} = 0.97$ and $\Delta E_P = 0.085$ V. These negative values for the $[Co^{III/II}H_3\mathbf{1}(OH)]^{1-/2-}$ and $[Fe^{III/II}H_3\mathbf{1}(OH)]^{1-/2-}$ couples reflect the highly negative primary coordination sphere provided by $[H_3\mathbf{1}]^{3-}$ and the hydroxo ligand. Irreversible redox processes are observed at more positive potentials. E_{pa} values of −0.10, 0.39, and 0.82 V vs SCE occur for $[Co^{II}H_3\mathbf{1}(OH)]^{2-}$, while for $[Fe^{II}H_3\mathbf{1}(OH)]^{2-}$, they are at 0.54 and 0.80 V vs SCE. The identity of the products from these oxidative processes is currently under investigation.

Summary and Conclusions

This work describes synthetic methods for synthesizing monomeric M−OH complexes using the tripodal ligand $H_6\mathbf{1}$ and water. Three equivalents of base are necessary to generate $[H_3\mathbf{1}]^{3-}$, which can bind a metal ion. Complexes of the type $[M^{II}H_3\mathbf{1}(OH)]^{2-}$ are obtained after addition of water with the H-bond cavity surrounding the M^{II}−OH unit. However, this route (method A) only gave complexes in yields of ≤40%. Substantially higher yields (50−70%) were obtained via method B that uses 4 equiv of base prior to the addition of H_2O. This extra base equivalent is proposed to deprotonate one of the α′-NH groups to afford a cavity having one basic site. The resulting α′-N^- group serves to scavenge the proton produced in the formation of $[M^{II}H_3\mathbf{1}(OH)]^{2-}$. The dual function of the synthetic cavity in these complexes resembles those found in metalloproteins, in which both H-bonds and general basic sites are used to control structure and function.

X-ray diffraction studies on the $[M^{II/III}H_3\mathbf{1}(OH)]^{2-/1-}$ complexes reveal that they have trigonal bypyramidal coordination geometry. The superstructure of the cavity provided by $[H_3\mathbf{1}]^{3-}$ has N−H bonds directed "inward", toward the M−OH unit. For the $[M^{II}H_3\mathbf{1}(OH)]^{2-}$ complexes, the M^{II}−OH bond lengths are longer than those reported for other synthetic monomeric complexes which lack the H-bonds to the hydroxo oxygen. However, the Zn^{II}−OH distance is similar to that observed in the active CAII. Extensive H-bonding to the Zn−OH unit also exists in the active site of this enzyme. Furthermore, the molecular structures of $[M^{II/III}H_3\mathbf{1}(OH)]^{2-/1-}$ complexes show

(29) Buckingham, D. A.; Clark, C. R. In *Comprehensive Coordination Chemistry*; Wilkinson, G., Guillard, R.D., McCleverty, J. A., Eds.; Pergamon Press: New York, 1987; pp 635−900.
(30) (a) Ardon, M.; Bino, A. *Inorg. Chem.* **1985**, *24*, 1343−1347. (b) Ardon, M.; Bino, A.; Jackson, N. G. *Polyhedron* **1987**, *6*, 181−187.
(31) Drago, R. *Physical Methods in Inorganic Chemistry*; Saunders: Philadelphia, PA, 1977; Chapter 11.
(32) Examples of paramagnetic Co(III) complexes with TBP stereochemistry: (a) McAuliffe, C. A.; Godfrey, S. M.; Mackie, A. G.; Pritchard, R. G. *Angew. Chem., Int. Ed. Engl.* **1992**, *31*, 919−921. (b) Jaynes, B. S.; Ren, T.; Liu, S.; Lippard, S. J. *J. Am. Chem. Soc.* **1992**, *114*, 9670−9671.

that the H-bond cavities furnish sufficient steric constraints to prevent additional metal complexes from interacting with the M−OH centers. This has allowed for the isolation of $[Co^{II}H_3\mathbf{1}(OH)]^{2-}$ and $[Co^{III}H_3\mathbf{1}(OH)]^{1-}$, which represent the first structurally characterized examples of a monomeric $Co^{III/II}$ redox pair having trigonal bipyramidal stereochemistry.

Acknowledgment is made to the NIH (Grant GM50781) for financial support of this research. We thank Dr. Doug Powell for help in generating Figures 2 and 3 and Professor Mike Hendrich and Adina Golombek for determining the *E*/*D* value in the EPR spectrum of $[Fe^{III}H_3\mathbf{1}(OH)]^{1-}$.

Supporting Information Available: EPR spectra of $[Co^{II}H_3\mathbf{1}(OH)]^{2-}$ and $[Fe^{III}H_3\mathbf{1}(OH)]^{1-}$ and CIF files of X-ray structural data. This material is available free of charge via the Internet at http://pubs.acs.org.

IC010250W